Supporting Information

New insight into lignin aggregation guiding efficient synthesis and functionalization of lignin nanosphere with excellent performance

Liheng Chen[a,b,†]*, Si-Man Luo[a,†], Cong-Min Huo[a], Yun-Feng Shi[a], Jun Feng[c], Jing-Yi Zhu[a,]*, and Wei Xue[a,]*, Xueqing Qiu[b]

[a] Key Laboratory of Biomaterials of Guangdong Higher Education Institutes, Guangdong Provincial Engineering and Technological Research Center for Drug Carrier Development, Department of Biomedical Engineering, Jinan University, Guangzhou 510632, China

[b] School of Chemical Engineering and Light Industry, Guangdong University of Technology, Guangzhou 510006, China

[c] Key Laboratory of Biomedical Polymers of Ministry of Education & Department of Chemistry, Wuhan University, Wuhan 430072, China

* Corresponding Author E-mail: lihengchen@gdut.edu.cn, jyzhu@jnu.edu.cn, weixue_jnu@aliyun.com,

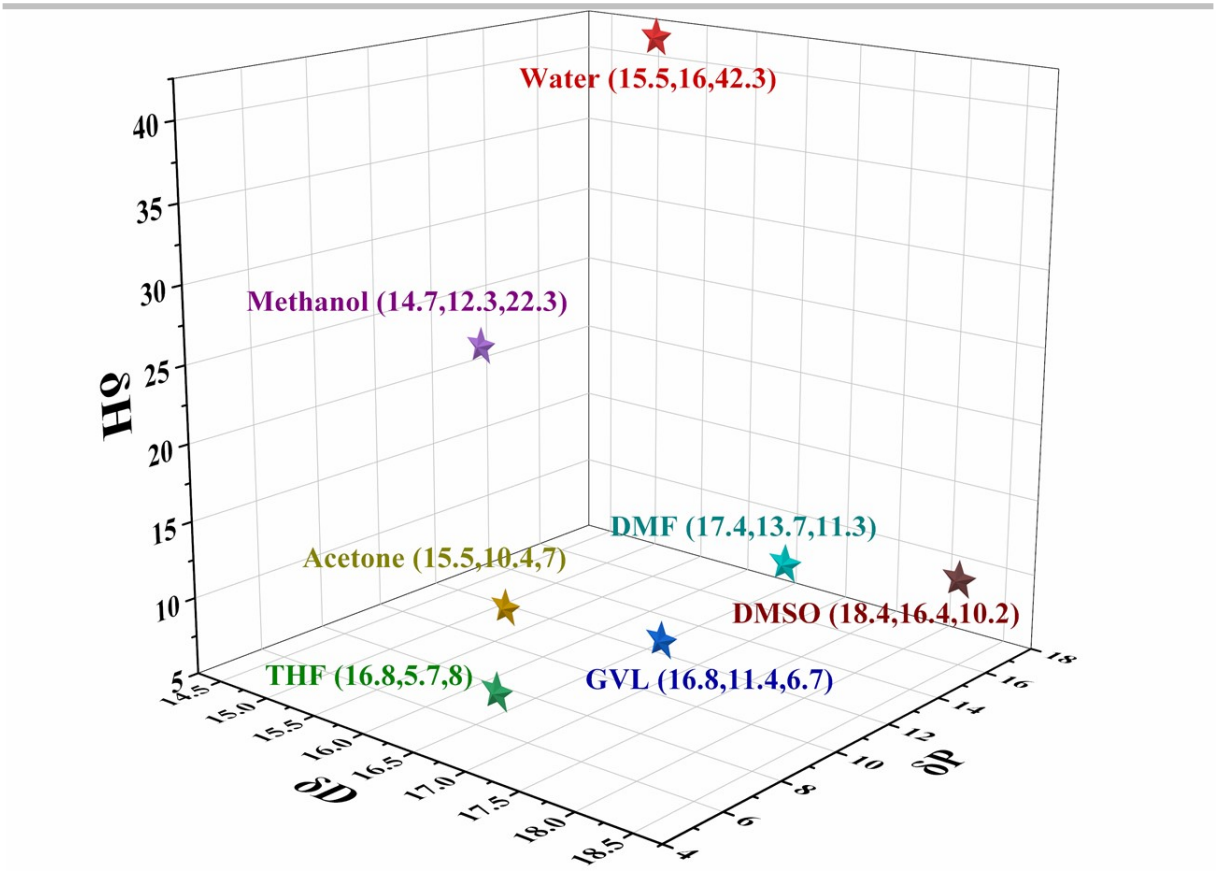

Figure S1. Hansen solubility parameters (HSP) of solvents obtained from HSPiP software.

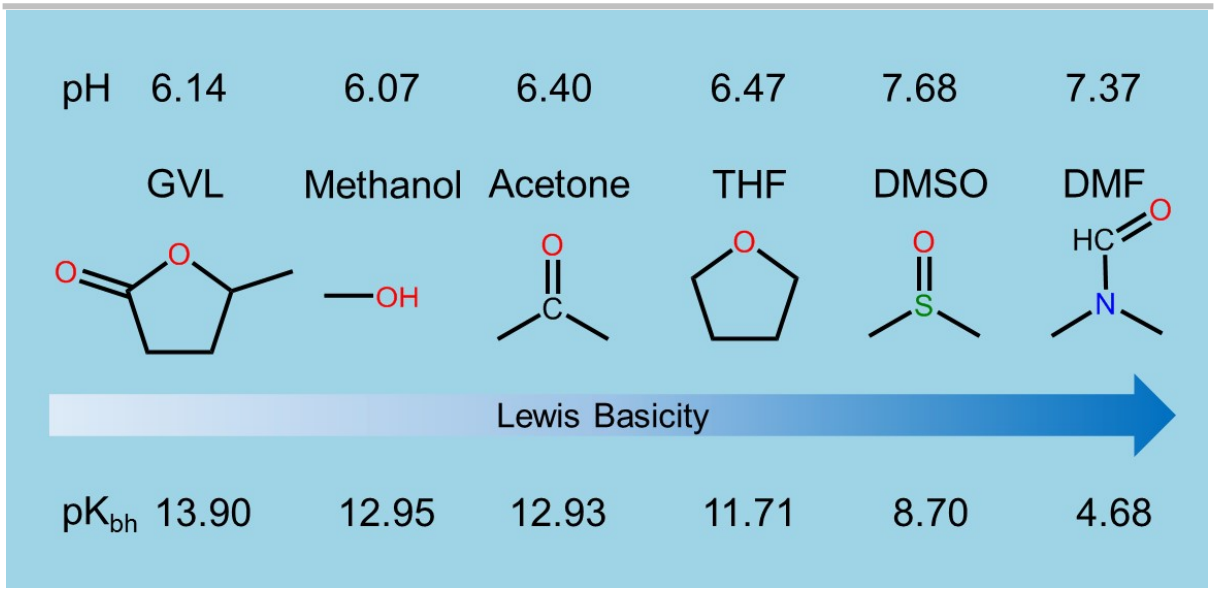

Figure S2 pH value of lignin solution (40 mg/mL) in different solvents (organic solvent/water with the volume ratio of 4:1) determined by a pH meter (Starter 2100, OHAUS Instruments (Shanghai) Co.,Ltd. China) and the abilities (pK_{bh}) of solvents binding hydrogen calculated by DFT.

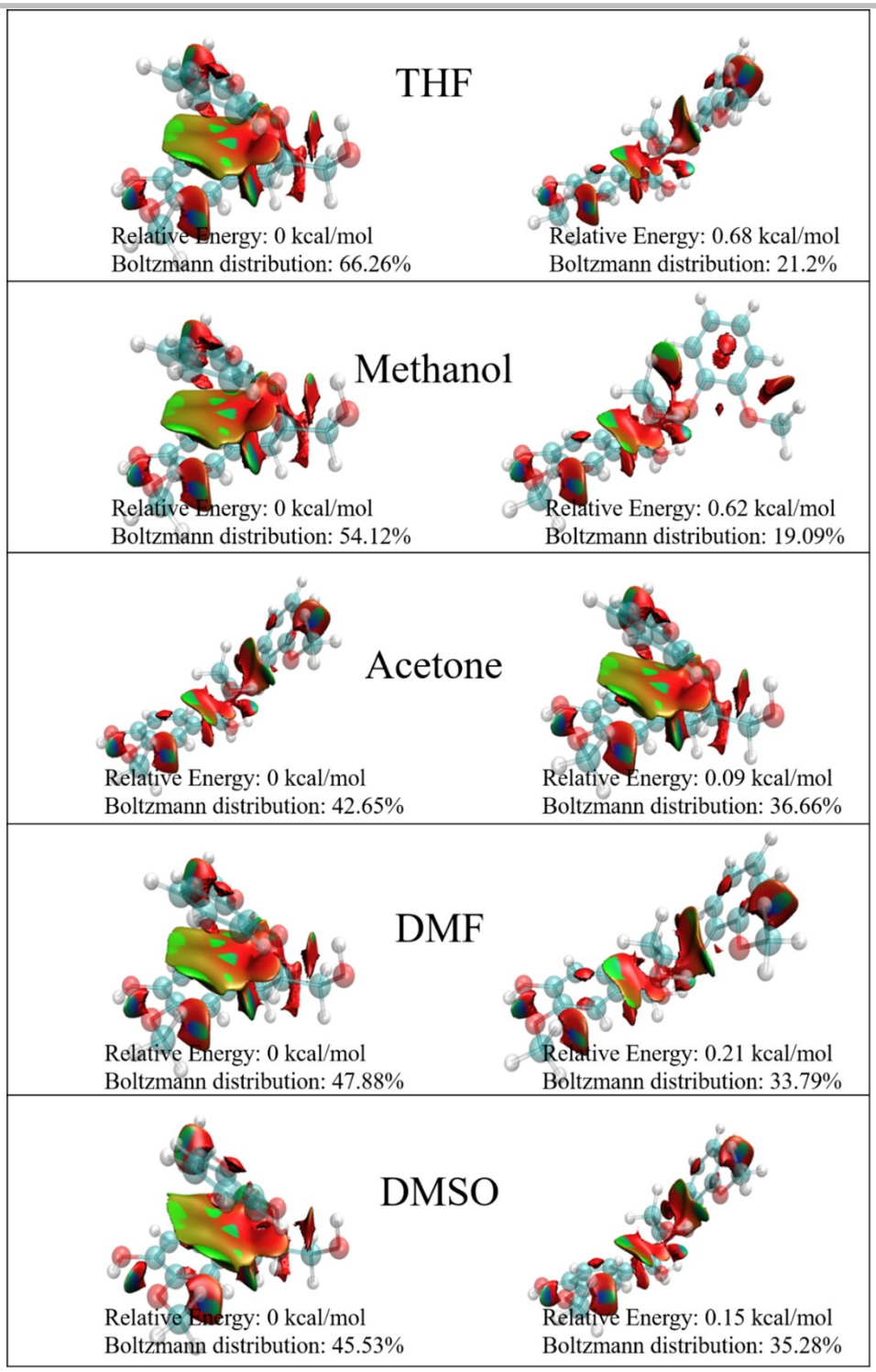

Figure S3. Isosurface (value=0.5) of reduced density gradient (RDG) of GGE configurations with the two lowest energies, respectively, in different implicit solvent models (GGE: CPK model, C-cyan, H-white, O-red).

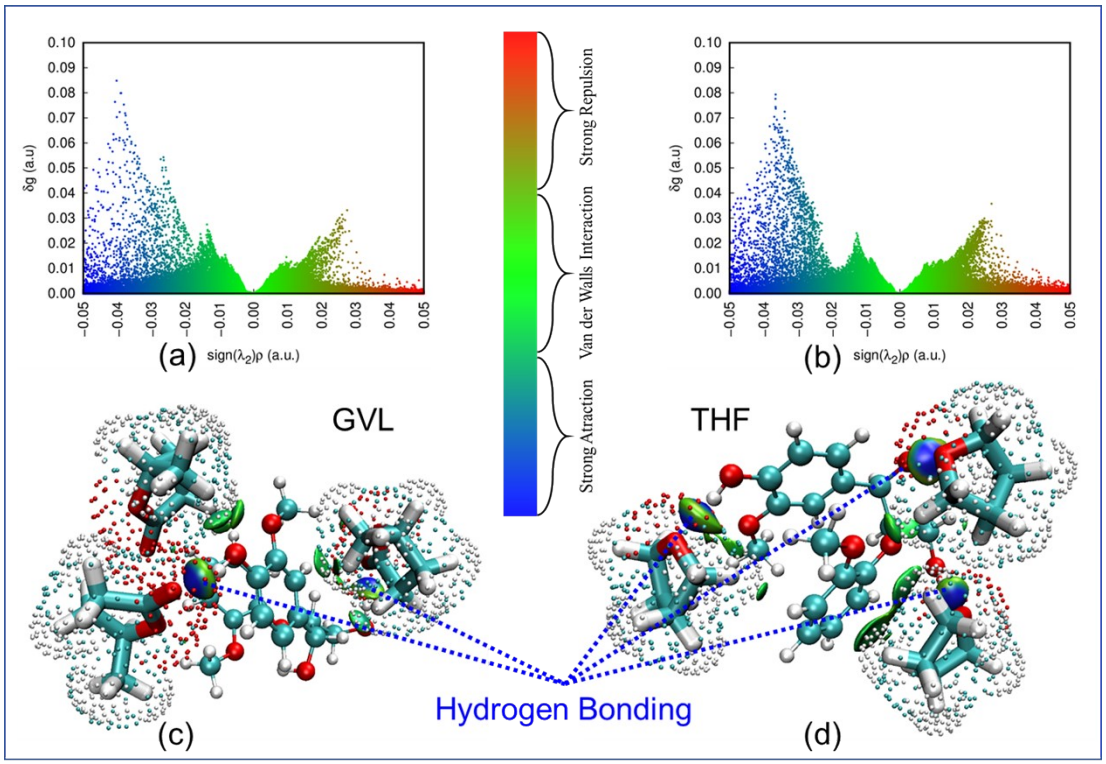

Figure S4. (a and b) Scatter graph and (c and d) isosurface (value=0.01 a.u.) of δg inter of GGE/solvent clusters based on independent gradient model (IGM) under implicit water model, respectively (GGE: CPK model; solvent molecules: solvent and licorice model, C-cyan, H-white, O-red).

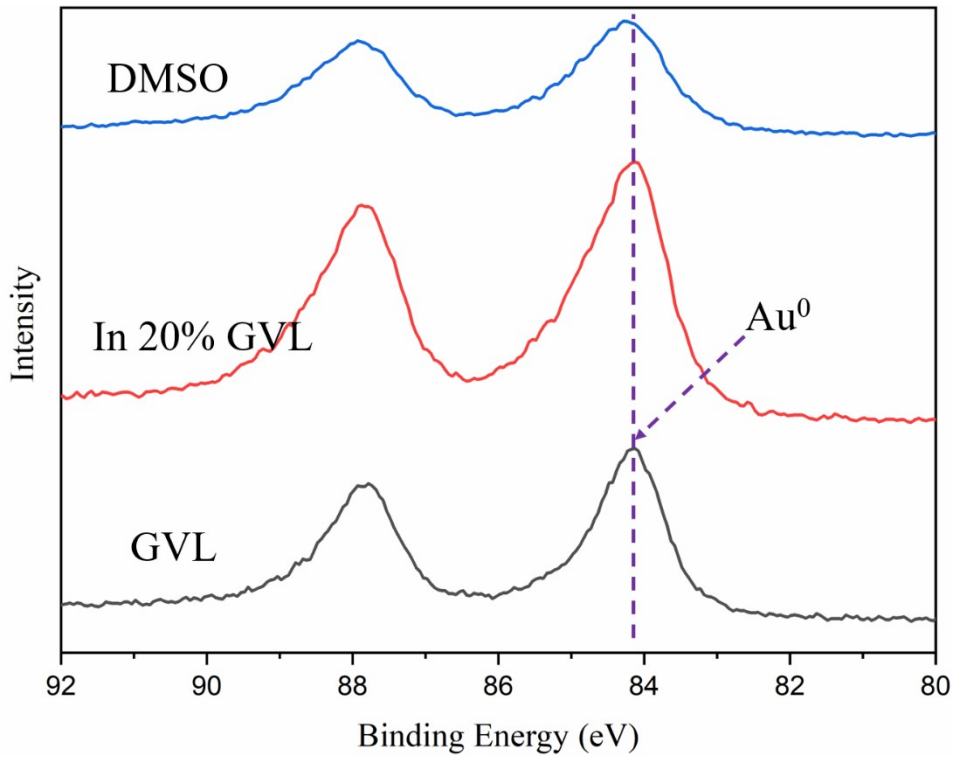

Figure S5. XPS spectra of Au-LNPs produced from GVL and DMSO, and the GVL-lignin solution dropped into 20% GVL solution.

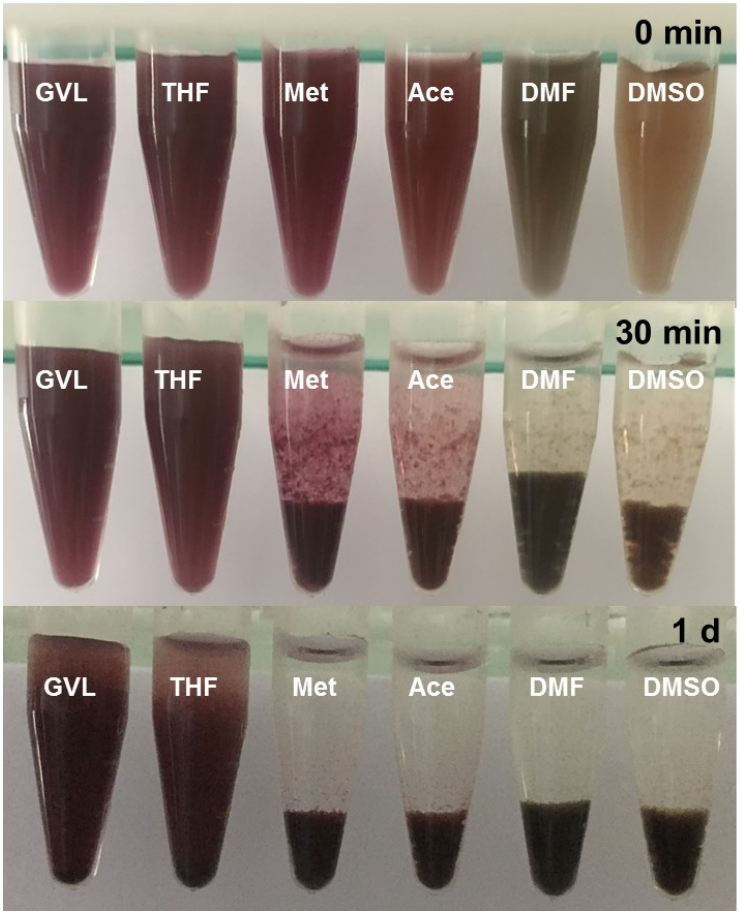

Figure S6. Images of obtained Au-LNPs from different solvents standing for different time.

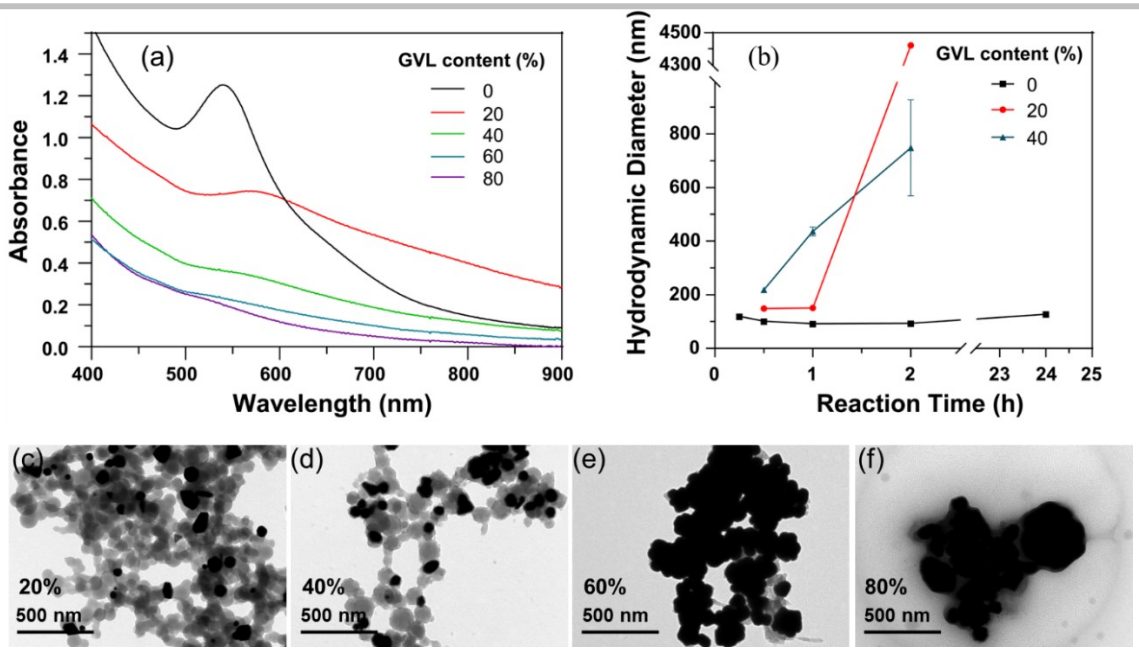

Figure S7. (a) UV-Visual spectra, (b) hydrodynamic diameters, and (c-f) TEM images of Au-LNPs from GVL-lignin solution dropped into GVL/water binary solvents with different GVL volume contents.

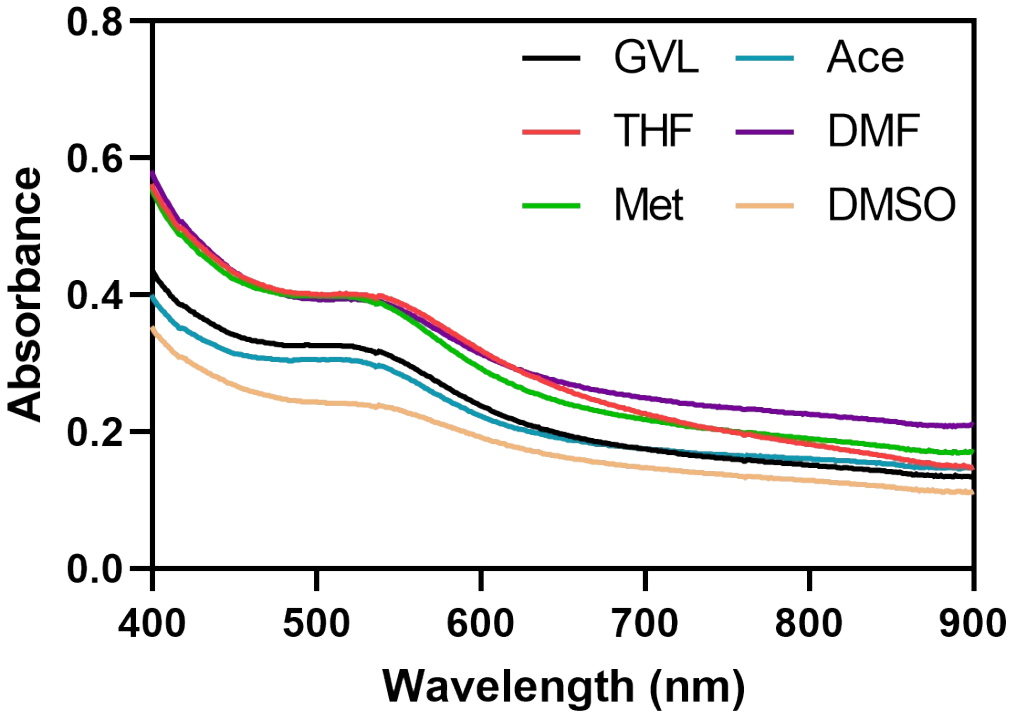

Figure S8. UV-Visual spectra of AuNPs produced from different solvents using ferulic acid as a reducing agent.

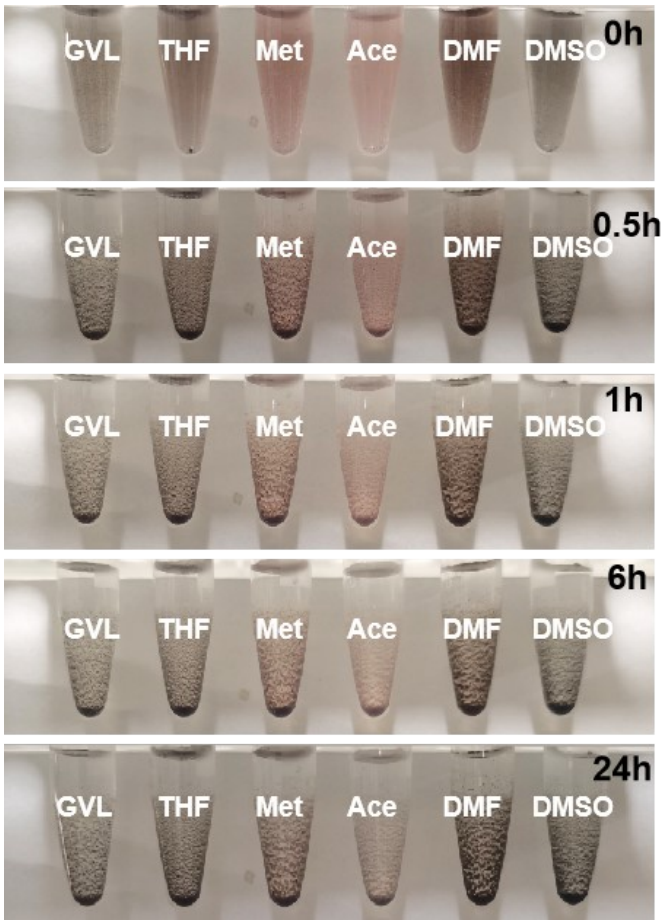

Figure S9. Images of AuNPs produced from different solvents using ferulic acid as a reducing agent standing for different time.

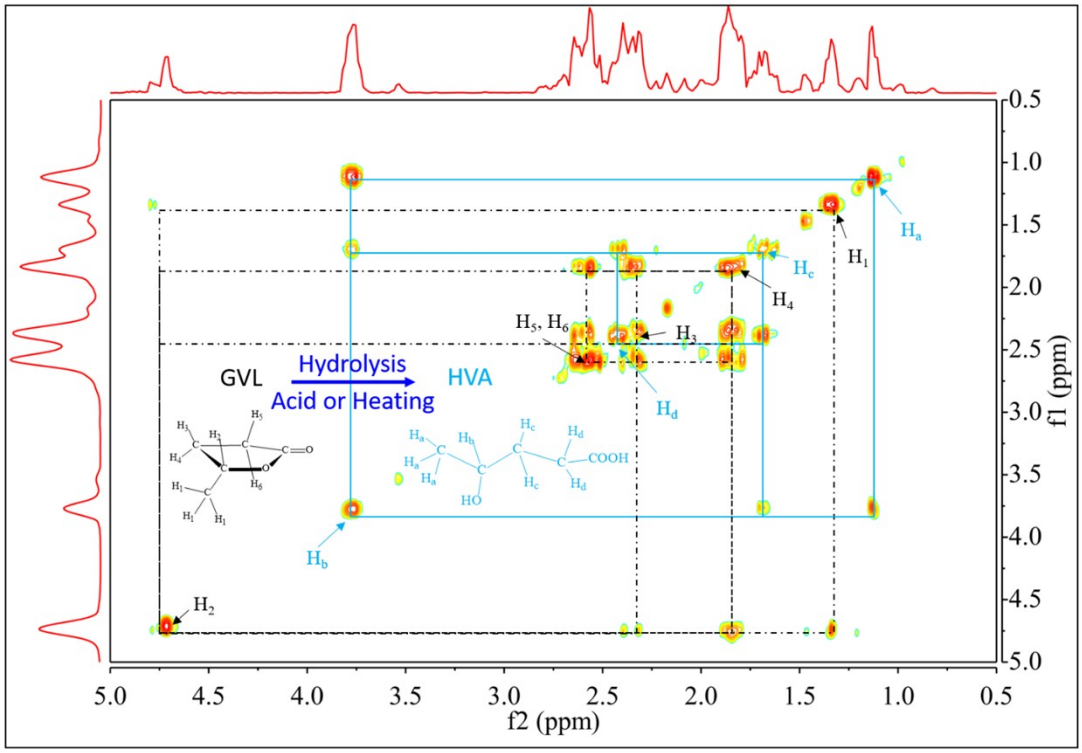

Figure S10. COSY-NMR of GVL and HVA detected by a Bruker AVANCEIII 500M NMR Spectrometer. NMR tube contained 1 mM chloroauric acid and 50 uL GVL in 0.8 mL D_2O was incubated at 30 ^oC for 2 h before the determination.

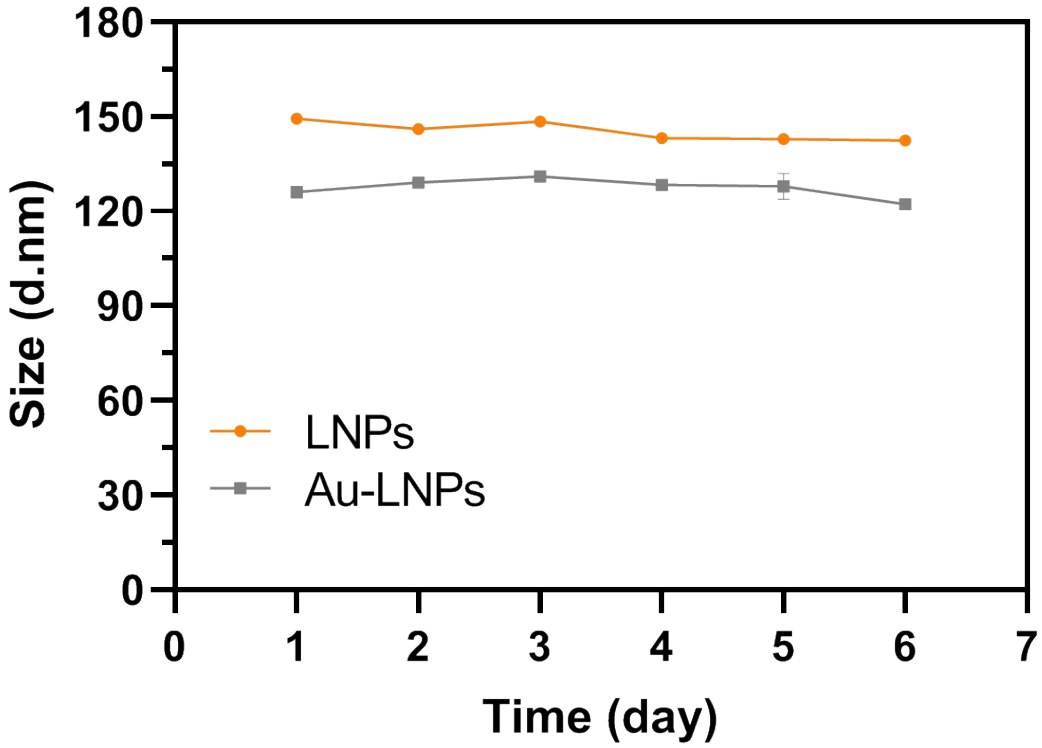

Figure S11. Time-dependent hydrodynamic diameters of different nanoparticles.

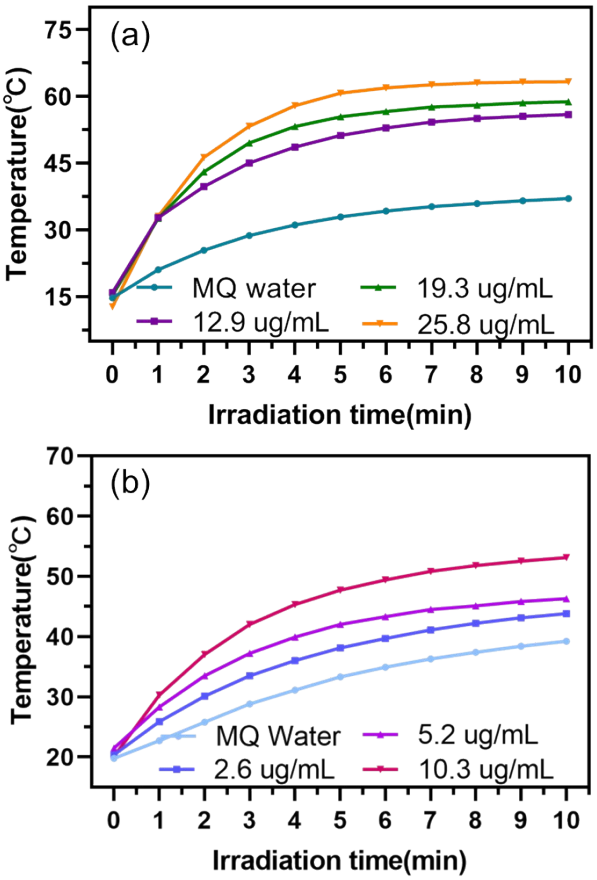

Figure S12. Heating profiles of Au-LNPs at different Au concentrations irradiated with an 808 nm laser power (2.5 W/cm^2), and (b) a 660 nm laser power (1.2 W/cm^2), respectively.